Chitosan Nanofibrous Scaffold Fabricated via Electrospinning: The Effect of Processing Parameters on the Nanofiber Morphology

T. Mazoochi [a] & V. Jabbari [b]

[a] Department of Surgery, Faculty of Medicine, Kashan University of Medical Science , Kashan, I. R. Iran

[b] Institute of Nanoscience and Nanotechnology, University of Kashan , Kashan, I. R. Iran
Published online: 26 Jul 2011.

PLEASE SCROLL DOWN FOR ARTICLE

CHITOSAN NANOFIBROUS SCAFFOLD FABRICATED VIA ELECTROSPINNING: THE EFFECT OF PROCESSING PARAMETERS ON THE NANOFIBER MORPHOLOGY

T. Mazoochi[1] and V. Jabbari[2]

[1]*Department of Surgery, Faculty of Medicine, Kashan University of Medical Science, Kashan, I. R. Iran*

[2]*Institute of Nanoscience and Nanotechnology, University of Kashan, Kashan, I. R. Iran*

Chitosan nanofibers were electrospun by using chitosan and triflouroacetic acid (TFA) solution as a solvent. Morphological characteristics of chitosan nanofibers fabricated by the electrospinning technique in different applied voltages (15–25 kV) and tip-to-collector distances (TCD) (5–15 cm) were examined using scanning electron microscopy (SEM). SEM images of electrospun nanofibers showed that morphology and diameter of the nanofibers were mainly affected by applied voltage. It also has shown that TCD directly affects spinnability and fiber diameter and at a very small distance (5 cm) droplets were formed due to electrospraying. The mechanical, thermal, and physicochemical properties of the chitosan nanofibrous membranes were investigated by tensile testing, TGA, porosimetry, and FT-IR analyses, respectively.

Keywords: Chitosan; Electrospinning; Nanofibers; Nanofibrous scaffold

INTRODUCTION

Chitin, composed of (1,4)-linked N-acetyl-β-D-glucosamine, is the second most abundant natural polymer in the world; it is primarily obtained from shrimp and crab shells. When degree of deacetylation (DD) of chitin reaches approximately 50%, it become soluble in aqueous acidic solution and is called chitosan (Figure 1). Chitosan has a repeated structure of (1,4)-linked β-D-glucosamine and has an intrinsic pK_a of ~6.5. The commercial products are traditionally composed of 80% β-D-glucosamine and 20% N-acetyl-β-D-glucosamine.[1]

Chitosan is generally soluble at pH below 6, and its solution properties depend on the molecular weight, degree of acetylation, and distribution of acetyl groups in the backbone.[2,3] Chitosan is a cationic polymer and has been used widely in food, cosmetic, biomedical, and pharmaceutical applications.[4–7] In particular, chitin and chitosan have been extensively used in many biomedical applications due to their (1) biodegradability and biocompatibility, (2) cellular binding capability, (3) acceleration
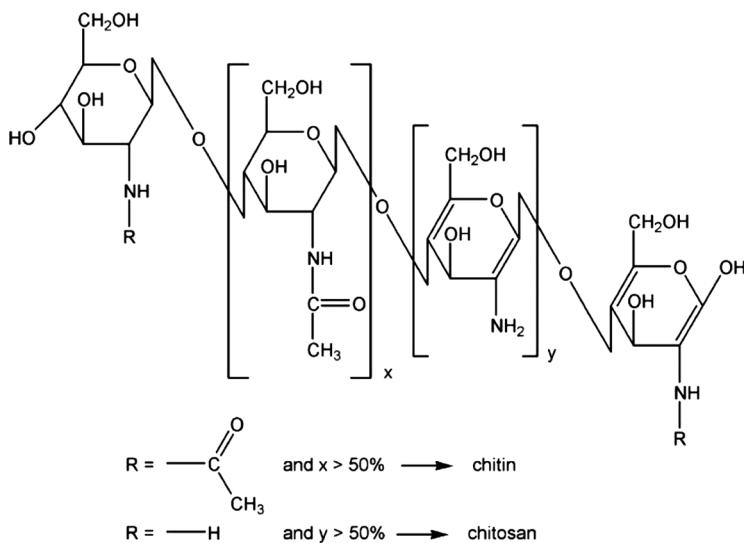
Figure 1. Chemical structure of chitin and chitosan.

of wound healing, (4) hemostatic properties, and (5) antifungal and anti-bacterial properties. A large variety of useful forms, including films, beads, sponges, tubes, powders, and fibers, can be obtained from chitosan.[8] Chitosan is degraded by enzymes, such as chitosanase and lysozyme, and its degradation rate is dependent on the temperature, ionic strength, and pH of the medium *in vitro*.[9] In general, the lower degree of acetylation of chitosan results in faster degradation rate of chitosan. Chitosan has also been proven to be biodegradable when implanted into animal bodies.[10]

Several fabrication methods for nanofibers, including drawing,[11] template synthesis,[12] phase separation,[13] self-assembly,[14] and electrospinning,[15] have been developed. Among these, the electrospinning process has become the most attractive because it is cost-effective, highly productive, and applicable to a variety of polysaccharides. Electrospinning is a technique that provides a promising and straightforward way to fabricate infinite and continuous nanofibers applied as nanostructured and biomedical materials.[16–21] A wide range of materials such as engineered polymers, biological polymers, ceramics, and composites has been successfully electrospun into one-dimensional materials having many different microstructures.[22–24] Applications of electrospun materials in nanotechnology include tissue scaffolds, drug delivery, composite reinforcement, chemical sensing, enzyme immobilization, membrane-based filtration, protective clothing, catalysis, solar cells, electronic devices, and others.[25–30]

Electrospinning involves application of electrostatic force instead of mechanical force to atomize a liquid solution into charged aerosol jets.[31] In a typical process, first a precursor solution is held at the tip of a nozzle in the form of a droplet by its surface tension, and then a charge is induced on the surface of the droplet when a high voltage is applied to the metallic nozzle. Finally, with an increase of electric field above a critical voltage for which the electro-hydrodynamic force within the charged droplet is larger than its surface tension, the droplet is distorted and a jet will erupt from the apex of a conical meniscus, commonly known as the Taylor cone.[32]

The charged jets move toward the collector while most of the solvents evaporate, resulting in solid fiber materials.[33]

In this work, we fabricated nanofibrous scaffolds using the natural polymer chitosan. We controlled the uniformity, diameter, and morphology of nanofibers by applied electric field strength and distance between the spinneret and the collecting plate.

MATERIALS AND METHODS

Electrospinning of Chitosan Nanofibers

Chitosan (Mw = 200,000, degree of deacetylation: 85%, Acros) and trifluoroacetic acid (TFA) (99%, Merck) were used as-received without further purification. Electrospinning of the chitosan was conducted using a 6% (w/v) chitosan solution in TFA. The complete electrospinning apparatus consisted of a syringe and stainless needle, a ground electrode, a copper plate covered by aluminum foil as a collector, and an adjustable high voltage supply (FNM, Iran) (Figure 2). The prepared solution was placed in the syringe, and the positive voltage lead from the power supply was attached to the external surface of the metal needle. When high positive voltage was applied across the source solution and the grounded collector, the solutions in the syringe would be ejected from the tip of the needle to generate nanofibers, which would be collected on the grounded collector. In this study, the chitosan solutions were electrospun at 15–25 kV positive voltage, TCD of 5–15 cm, and 0.5 mL/h solution flow rate controlled by a syringe pump.

Characterizations

The surface morphology of the chitosan nanofibers was observed on a JEOL JSM-5600LV scanning electron microscope (SEM) at an acceleration voltage of
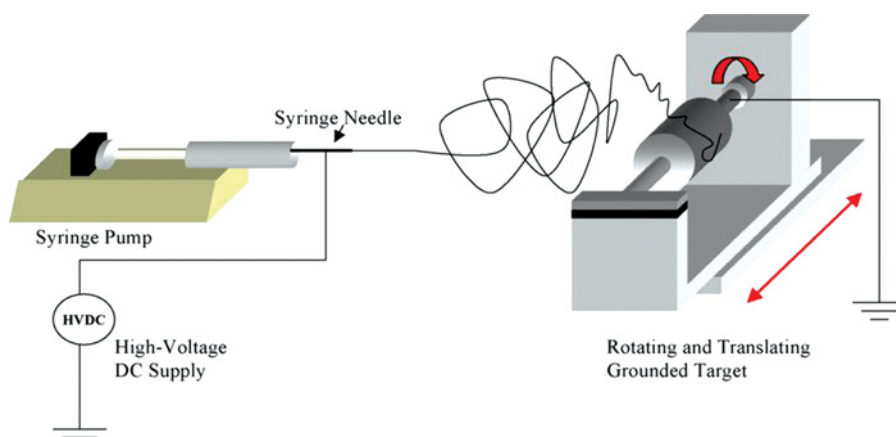

Figure 2. Generic electrospinning setup depicting the major components of the electrospinning process, including a high-voltage power supply, polymer solution, and grounded collection target (color figure available online).

10–15 kV. Samples for SEM were dried under vacuum, mounted on metal stubs, and sputter-coated with gold. The mean fiber diameters were estimated using image analysis J software and calculated by selecting about 100 fibers randomly observed on the SEM image.

The samples that were used for Fourier transform-infrared (FT-IR) measurements were cast to be thin enough to ensure that the observed absorption was within the linearity range of the detector. FT-IR spectra of the nanofibers mats were recorded using attenuated total reflection (ATR) in an IR spectrometer (Nicolet Avatar 360, Madison, Wis., USA). The transmission infrared spectra of all samples exhibited broad peaks in a range from 400 to 4000/cm.

Thermal stability of the electrospun mats was examined by thermogravimetric (TGA) experiments using an SII model EXTAR TG 6200. All the samples were pre-weighed and allowed to undergo the programmed heating in the temperature range of 23°–600°C at a rate of 10°C/min.

Tensile properties of electrospun nanofibrous membranes were determined using a universal testing machine (Testmetric M350-20KN, UK) equipped with a 100 N load cell at a cross-head speed of 5 mm/min in the ambient environment. The gauge length of tensile samples was 40 mm. The samples were prepared in rectangular shape with dimensions of $60 \times 10 \, mm^2$ from dry electrospun nanofibrous membranes. The samples were then taken out of the bottles and tested under tension. The tensile moduli that are presented in this article are averaged results of five tests.

Pore diameter distribution, total pore volume, pore area, and porosity of the matrix were measured by an AutoPore IV 9500 V1.05 mercury apparatus (Micrometritis Instrument Co., Germany).

RESULTS AND DISCUSSIONS

Morphological Properties of Nanofibers

The properties of the polymer solution (such as surface tension, viscosity, and solvent) have a significant influence in the electrospinning process and resultant fiber morphology. Other important parameters that affect the electrospinning process are various external factors exerting on the electrospinning jets. This includes the voltage supplied, feed rate, temperature of solution, type of collector, diameter of the needle, and distance between the needle tip and collector. These parameters have a definite influence in the fiber morphology, even more than the solution parameters. In this study, we change the electric field strength and distance between the spinneret and the collecting plate to control the morphology and diameter of chitosan nanofibers (Table I).

Distance Between Tip and Collector (TCD)

In most cases, the flight time as well as the electric field strength will affect the electrospinning process and the resultant fibers. Varying the TCD will have direct influence on both the flight time and the electric field strength. For independent fibers to form, the electrospinning jet must be allowed enough time for most of the solvent to be evaporated. When the TCD is reduced, the jet will have a shorter

Table I. Processing parameters of electrospinning of chitosan nanofiber

Trial no.	V (kv)	TCD (cm)	C (w/v)	F (mL/min)	S (rpm)	Average fiber diameter (nm)
1	15	5	8	0.5	1000	beads
2	15	10	8	0.5	1000	beads
3	15	15	8	0.5	1000	220
4	20	5	8	0.5	1000	190
5	20	10	8	0.5	1000	210
6	20	15	8	0.5	1000	280
7	25	5	8	0.5	1000	160
8	25	10	8	0.5	1000	180
9	25	15	8	0.5	1000	280

V: voltage; TCD: spinning distance; F: flow rate of solution; C: concentration; S: speed of rotating collector.

distance to travel before it reaches the collector plate. Moreover, the electric field strength also will increase at the same time, and this will increase acceleration of the jet to the collector. As a result, there may not be enough time for the solvent to evaporate when it hits the collector and fiber diameter increases. When the distance is too small, excess solvent may cause the fibers to merge where they contact to form junctions, resulting in inter- and intra-layer bonding.[36] This interconnected fiber mesh may provide an additional strength to the resultant scaffolds. On the other hand, if the TCD is too long, the strength of the electric field becomes so weak that the fiber diameter increases.[37,38]

Figure 3 shows the morphology and average diameter of the electrospun nanofibers at different TCDs. When the TCD was 5 cm, the distance between tip and collector was so short that the instability of the jet increased and the spinning solution could not be fully stretched, resulting in an increase of nanofiber diameter and the formation of beads. It is presumed that if the TCD is too high it weakens the strength of the electric field, resulting in an increase of nanofiber diameter.

Applied Voltage

A crucial element in electrospinning is the application of a high voltage to a solution. The high voltage will induce necessary charge on the solution and, together with the external electric field, it will initiate the electrospinning process when the electrostatic force in the solution overcomes the surface tension of the solution. Generally, either high positive or negative voltage of more than 6 kV is able to cause the solution drop at the tip of the needle to distort into the shape of a Taylor cone during jet initiation.[39] Depending on the feed rate of the solution, a higher voltage may be required so that the Taylor cone is stable. The coulombic repulsive force in the jet will then stretch the visco-elastic solution. If the applied voltage is higher, the greater amount of charge will cause the jet to accelerate faster and a greater volume of solution will be drawn from the tip of the needle. This may result in smaller and less stable Taylor cone.[40] When the drawing of the solution to the collection plate is faster than that supplied from the source, the Taylor cone may recede into the needle.[37]
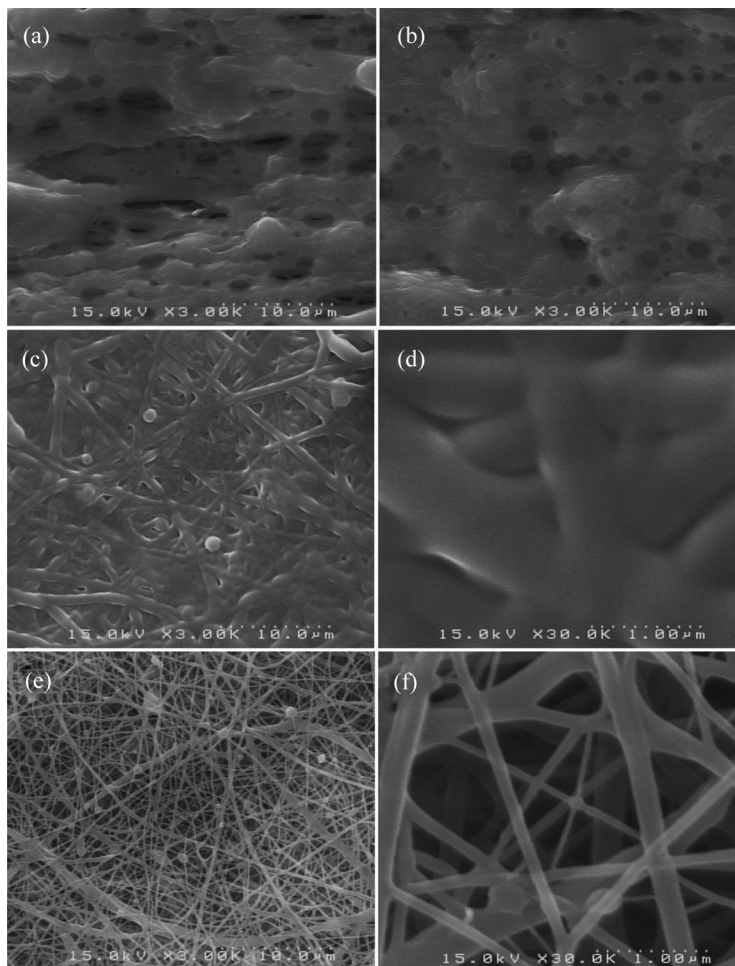
Figure 3. SEM images of chitosan fibers at TCD of: (a), (b) 5 cm; (c), (d) 7 cm; and (e), (f) 10 cm. In all experiments V = 15 kV, C = 8% (w/v), S = 1000, and F = 0.5 (mL/min). The difference between the pairs (a) and (b), (c) and (d), and (e) and (f) is their magnification.

As both the voltage supplied and the resultant electric field have an influence on the stretching and acceleration of the jet, they will have an influence on the morphology of the obtained fibers. In most cases, a higher voltage will lead to greater stretching of the solution due to the greater coulombic forces in the jet as well as due to the stronger electric field. These have the effect of the reducing the diameter of the fibers[36] and also encourage faster solvent evaporation to yield drier fibers.[41–43] Given the increased stretching of the jet due to the higher voltage, there should be less bead formation, as shown in Figure 4.[44]

Concerning the applied voltages investigated, it also should be mentioned that chitosan is difficult to electrospin into a fibrous structure because it has a polycationic character in an acidic aqueous solution due to many amino groups in its backbone. Its polycationic nature excessively increases the surface tension of the solution. High

electrical force is thus required to produce the electrospun chitosan nanofibers, and particles are often formed during the electrospraying process, likely due to the repulsive forces between ionic groups in the chitosan backbone in the acidic solution.[45]

As compared between Figures 4 and 5, the uniformity of the chitosan nanofibers formed increased with increasing voltage at significant levels. Subsequent analysis of the individual groups resulted in significant differences for both nanofiber diameter and uniformity (Figure 6).

Physicochemical and Mechanical Characterization of Nanofibers

Characterization of chitosan nanofibrous membrane is undertaken primarily to correlate test measurements of the useful properties of this material and also to

Figure 4. SEM images of chitosan fibers at TCD of: (a), (b) 5 cm; (c), (d) 7 cm; and (e), (f) 10 cm. In all experiments V = 20 kV, C = 8% (w/v), S = 1000, and F = 0.5 (mL/min). The difference between the pairs (a) and (b), (c) and (d), and (e) and (f) is their magnification.
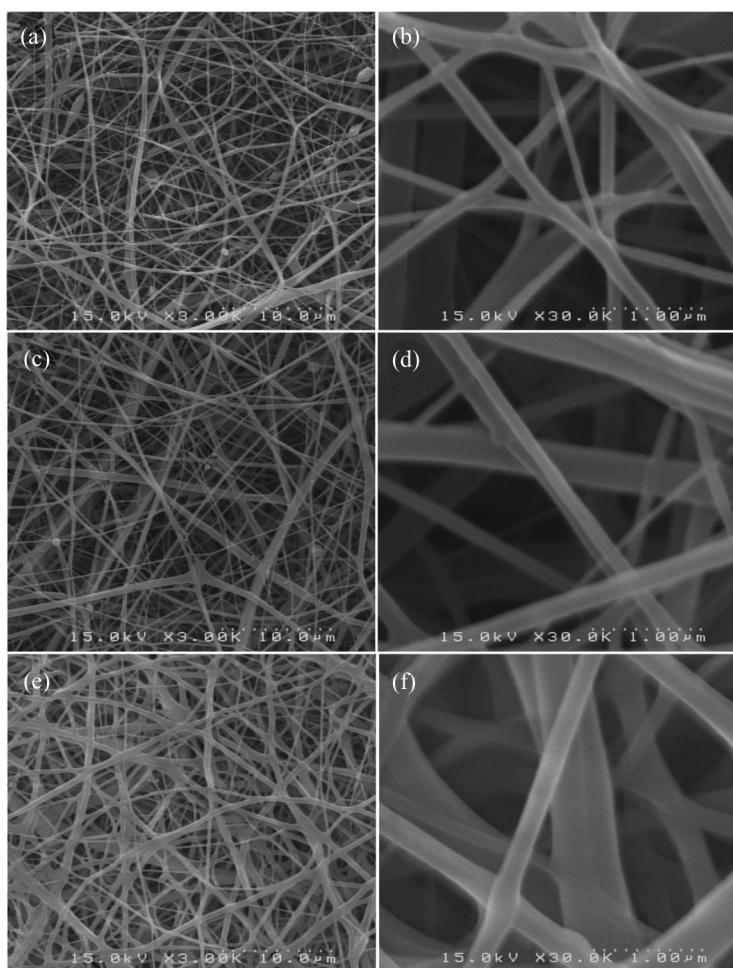
Figure 5. SEM images of chitosan fibers at TCD of: (a), (b) 5 cm; (c), (d) 7 cm; and (e), (f) 10 cm. In all experiments V = 25 kV, C = 8% (w/v), S = 1000, and F = 0.5 (mL/min). The difference between the pairs (a) and (b), (c) and (d), and (e) and (f) is their magnification.

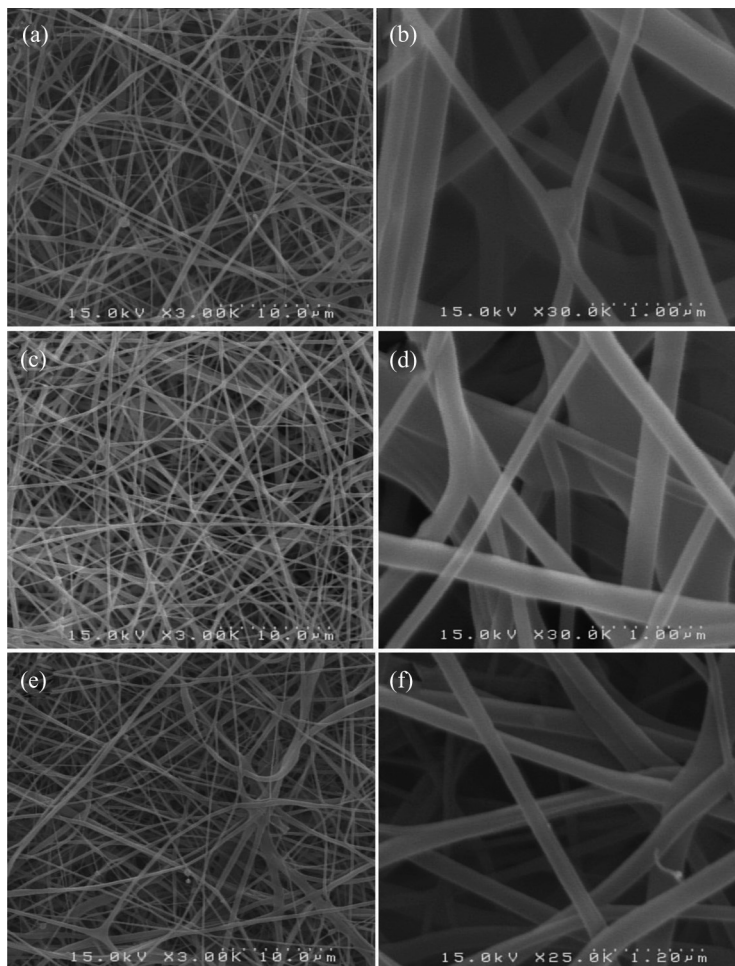ensure consistent high quality of the product during manufacture. In principle, there is a large number of different characterization techniques that can be used for nanofibers. In the following sections, selected characterization tests based on the several common anticipated uses of nanofiber materials are presented. The assessment of interstitial porosity properties, analysis of fiber chemical and physical structures, and mechanical integrity of electrospun chitosan nanofibrous membrane are the most important measurements in several application areas.

FT-IR spectroscopy. The FT-IR spectra of the electrospun chitosan nanofiber mat are presented in Figure 7; they show that the main characteristic peaks of chitosan are at $3420 \, cm^{-1}$ (the O–H stretching band), $2876 \, cm^{-1}$ (the C–H stretching band), $1598 \, cm^{-1}$ (the N–H bending band), $1424 \, cm^{-1}$ (the C–N stretching band),
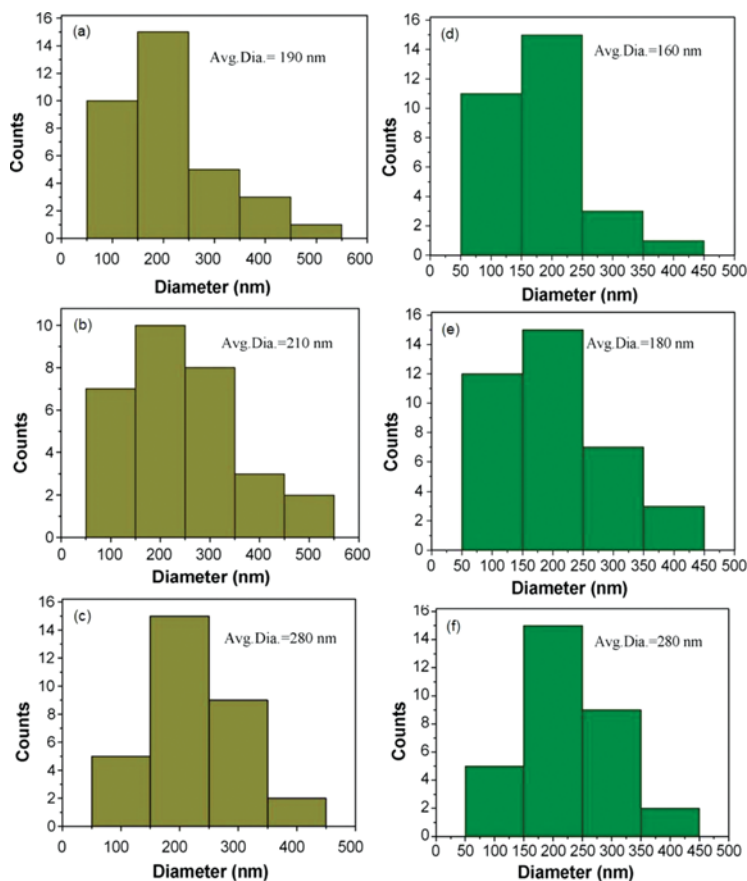
Figure 6. Fiber diameter distribution in the electrospun chitosan nanofibers fabricated in TCD = 5, 10, and 15 cm at applied voltages of 20 kV (a)–(c) and 25 kV (d)–(f) (color figure available online).

$1379 \, cm^{-1}$ (the bridge O stretching band), and $1084 \, cm^{-1}$ (the C–O stretching band).[34,35] It seems that the carbonyl (CO) stretching band disappeared by the wide N–H bending band that appeared at $1598 \, cm^{-1}$.

Thermal properties. The thermal decomposition of the chitosan nanofibrous membrane has been studied using thermal analysis. Figure 8 shows the TGA diagram for the elecrospun chitosan nanofibrous membrane. TGA showed two different stages of weight loss. The first stage ranges between 10° and 100°C. This may correspond to the loss of the adsorbed and bound water and acetic acid molecules. The second stage of weight loss starts at 280°C and continues up to 340°C, during which there was 64% weight loss due to the degradation of chitosan nanofibers.

Mat porosity. The pores play an important role in determining the physiochemical properties of porous substrates and have a deterministic effect on the performance of membranes, catalysts, adsorbents, and other uses. To design electrospun nanofibrous substrates for such applications, it is necessary to analyze the pore
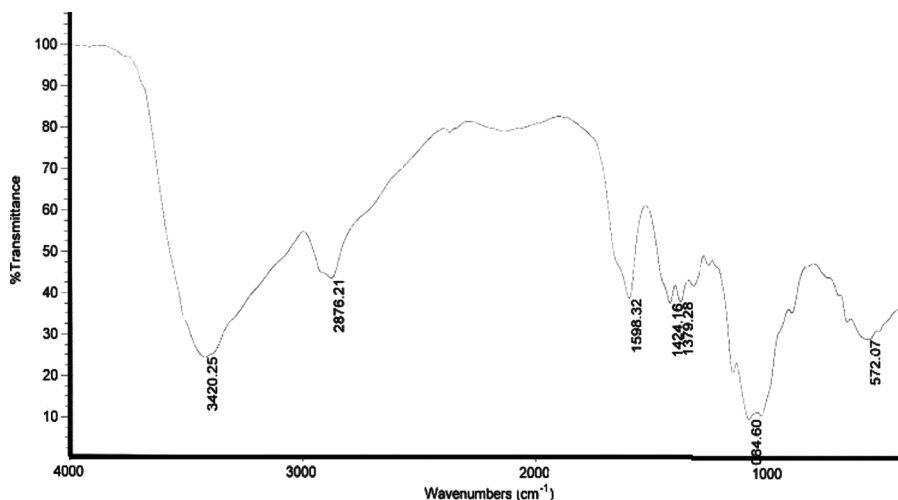
Figure 7. FT-IR spectra of chitosan.

size and porosity.[46] In general, in the key application area of tissue engineering, close control over the electrospun nanofiber mat porosity can be critical to success in viable scaffold development. Cellular ingress to the interior of nanofibrous scaffolds as well the efficacy of cell-nanofiber interactions leading to adhesion and proliferation of cells are well known to be related to porosity.[47] Based our results presented in Table II, as fiber diameter decreases, the electrospun chitosan mat porosity and surface area increase, which make the scaffold more useful for biomedical application.

Mechanical properties of mats. Electrospun polymer nanofibers have several possible applications such as filtration, tissue scaffolds, gas sensors, and protective clothing, among others. In order to meet requirements of long-life durability in those applications, mechanical properties of electrospun nanofibrous membranes
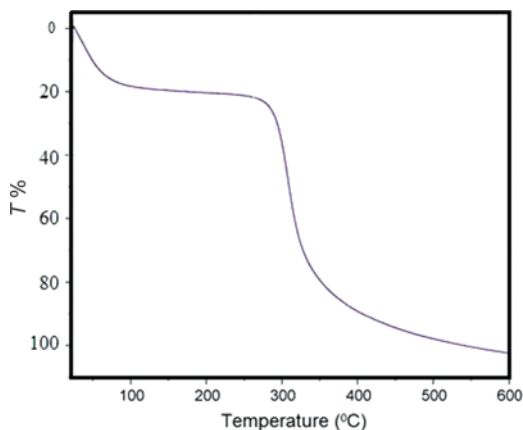

Figure 8. TGA diagram of chitosan nanofibers (color figure available online).

Table II. Pore characterization and modulus data illustrating the effect of electrospinning operating conditions on electrospun chitosan nanofiber mat characteristics

Sample no.	Average fiber diameter (nm)	Porosity (%)	Total pore area (m^2/g)	Pore diameter range (μm)	Tensile strength (MPa)
3	220	62	11	0.2–84	3.85
4	190	72	12	0.24–72	4.12
5	210	75	15	0.21–65	3.27
6	280	68	21	0.12–58	2.22
7	160	85	19	0.14–45	3.64
8	180	87	14	0.9–51	2.65
9	280	82	15	0.1–44	1.98

have to be known. Tensile properties of electrospun chitosan nanofibrous membranes in this work are summarized in Table II. As shown in Table II, for fibers with higher diameter, relatively higher modulus was observed for the electrospun chitosan membranes. Values of 3.85, 4.12, 3.27, 2.22, 3.64, 2.65, and 1.98 MPas were obtained for the tensile modulus of the chitosan fiber samples with average diameter of 160 to 280 nm. Based on our results given in Table II, further change in the mechanical properties was achieved by further applied voltage of the processing conditions. The chitosan electrospun mats are claimed to be mechanically robust and to have the capability to conform to motion and, thus, are compatible with tissue.[48,49]

CONCLUSION

This experiment showed that continuous individual electrospun chitosan nanofibers with diameters in the range of approximately 50 to 550 nm could be collected and that the applied voltage and TCD had significant effects on the fiber diameter and uniformity as confirmed by SEM. It was observed that fiber diameter decreased as applied voltage increased, and for TCD, inverse results were found. It has been shown that morphology of the electrospun nanofibers can be controlled by changing the electrospinning conditions. Also, the mechanical properties and pore characteristics of the nanofibrous chitosan membranes were systematically studied. Those electrospun fibers exhibit several interesting characteristics, e.g., a high surface area, a small interfibrous pore size with high porosity of the obtained fiber mat, and relatively high mechanical strength.

REFERENCES

1. Sandford, P. A., A. Steinnes, C. L. McCormick, and G. B. Butler. 1991. In *Water-Soluble Polymers: Synthesis, Solution Properties, and Applications*, eds. S. W. Shalaby, C. L. McCormick, and G. B. Butler, p. 430. Washington, D.C.: American Chemical Society.
2. Kubota, N., and Y. Eguchi. 1997. Facile preparation of water-soluble N-acetylated chitosan and molecular weight dependence of its water-solubility. *Polym. J.* 29: 123–127.
3. Aiba, S. 1991. Evidence for the presence of random and block copolymer structures in partially N-acetylated chitosan. *Int. J. Biol. Macromol.* 13: 40–44.
4. Hirano, S., H. Seino, Y. Akiyama, and I. Nonaka. 1990. In *Progress in Biomedical Polymers*, eds. C. G. Gebelein and R. L. Dunn, p. 283. New York: Plenum Press.

5. Winterowd, J. G., and P. A. Sandford. 1995. In *Food Polysaccharides and Their Applications*, ed. A. M. Stephen, p. 441. New York: Marcel Dekker.

6. Peter, M. G. 1995. Applications and environmental aspects of chitin and chitosan. *J. Macromol. Sci. Pure Appl. Chem.* A32: 629–640.

7. Rao, S. B., and C. P. Sharma. 1997. Use of chitosan as a biomaterial: Studies on its safety and hemostatic potential. *J. Biomed. Mater. Res.* 34: 21–28.

8. Rinaudo, M. 2006. Chitin and chitosan: Properties and applications. *Prog. Polym. Sci.* 31: 603–632.

9. Hirano, S., and H. Tsuchida. 1989. N,N-acetylation in chitosan and the rate of its enzyme-hydrolysis. *Biomaterials* 10: 574–576.

10. Tomihata, K., and Y. Ikada. 1997. *In vitro* and *in vivo* degradation of films of chitin and its deacetylated derivatives. *Biomaterials* 18: 567–575.

11. Hartgerink, K., M. Kotaki, Y. Z. Zhang, X. M. Mo, and S. Ramakrishna. 2004. Recent advances in polymer nanofibers. *J. Nanosci. Nanotechnol.* 4: 52–65.

12. Hulteen, J. C., H. X. Chen, C. K. Chambliss, and C. R. Martin. 1997. Template synthesis of carbon nanotube and nanofiber arrays. *Nanostruct. Mater.* 9: 133–136.

13. Ma, P. X., and R. Y. Zhang. 1999. Synthetic nano-scale fibrous extracellular matrix. *J. Biomed. Mater. Res.* 46: 60–72.

14. Hartgerink, J. D., E. Beniash, and S. I. Stupp. 2002. Peptide-amphiphile nanofibers: A versatile scaffold for the preparation of self-assembling materials. *Proc. Natl. Acad. Sci. U.S.A.* 99: 5133–5138.

15. Reneker, D. H., and I. Chun. 1996. Nanometre diameter fibres of polymer produced by electrospinning. *Nanotechnology* 7: 216–223.

16. Huang, Z. M., Y. Z. Zhang, M. Kotaki, and S. Ramakrishna. 2003. A review on polymer nanofibers by electrospinning and their applications in nanocomposites. *Compos. Sci. Technol.* 63: 2223.

17. Li, D., and Y. N. Xia. 2004. Direct fabrication of composite and ceramic hollow nanofibers by electrospinning. *Adv. Mater.* 16: 1151.

18. Reneker, D. H., and I. Chun. 1996. Nanometre diameter fibres of polymer produced by electrospinning. *Nanotechnology* 7: 216.

19. Nair, L. S., S. Bhattacharyya, and C. T. Laurencin. 2004. Development of novel tissue engineering scaffolds via electrospinning. *Expert Opin. Biol. Ther.* 4: 659.

20. Pham, Q. P., U. Sharma, and A. G. Mikos. 2006. Electrospinning of polymeric nanofibers for tissue engineering applications: A review. *Tissue Eng.* 12: 1197.

21. Pan, H., L. M. Li, L. Hu, and X. J. Cui. 2006. Continuous aligned polymer fibers produced by a modified electrospinning method. *Polymer* 47: 4901.

22. Dai, H. Q., J. Gong, H. Kim, and D. Lee. 2002. A novel method for preparing ultra-fine alumina-borate oxide fibres via an electrospinning technique. *Nanotechnology* 13: 674.

23. Yoon, K. H., K. S. Kim, X. F. Wang, D. F. Fang, B. S. Hsiao, and B. Chu. 2006. High flux ultrafiltration membranes based on electrospun nanofibrous PAN scaffolds and chitosan coating. *Polymer* 47: 2434.

24. Matthews, J. A., G. E. Wnek, D. G. Simpson, and G. L. Bowlin. 2002. Electrospinning of collagen nanofibers. *Biomacromolecules* 3: 232.

25. Murugan, R., and S. Ramakrishna. 2006. Nano-featured scaffolds for tissue engineering: A review of spinning methodologies. *Tissue Eng.* 12: 435.

26. Kim, J., H. F. Jia, and P. Wang. 2006. Challenges in biocatalysis for enzyme-based biofuel. *Biotechnol Adv.* 24: 296.

27. Jose, M. V., B. W. Steinert, V. Thomas, D. R. Dean, M. A. Abdalla, G. Price, and G. M. Janowski. 2007. Morphology and mechanical properties of Nylon 6/MWNT nanofibers. *Polymer* 48: 1096.

28. Qin, X. H., and S. Y. Wang. 2006. Filtration properties of electrospinning nanofibers. *J. Appl. Polym. Sci.* 102: 1285.

29. Wang, X. Y., C. Drew, S. H. Lee, K. J. Senecal, J. Kumar, and L. A. Samuelson. 2002. Explosive detection by fluorescent electrospun polymer membrane sensor. *J. Macromol. Sci. Pure Appl. Chem.* 39: 1251.

30. Ramakrishna, S., K. Fujihara, W. E. Teo, T. Yong, Z. W. Ma, and R. Ramaseshan. 2006. Electrospun nanofibers: Solving global issues. *Mater. Today* 9: 40.

31. Doshi, J., and D. H. Reneker. 1995. Electrospinning process and application of electrospun fibers. *J. Electrostat.* 35: 151.

32. Ganan-Calvo, A. M. 1997. Cone-jet analytical extension of Taylor's electrostatic solution and the asymptotic universal scaling laws in electrospraying. *Phys. Rev. Lett.* 79: 217.

33. Reneker, D. H., A. L. Yarin, H. Fong, and S. Koombhongse. 2000. Bending instability of electrically charged liquid jets of polymer solutions in electrospinning. *J. Appl. Phys.* 87: 4531.

34. Lim, S. H., and S. M. Hudson. 2004. Application of a fiber-reactive chitosan derivative to cotton fabric as an antimicrobial textile finish. *Carbohydr. Res.* 339: 313–319.

35. Mivehi, L., S. H. Bahrami, and R. A. Malek. 2008. Properties of polyacrylonitrile-N-(2-hydroxy)propyl-3-trimethylammonium chitosan chloride blend films and fibers. *J. Appl. Polym. Sci.* 109: 545–554.

36. Buchko, C. J., L. C. Chen, Y. Shen, and D. C. Martin. 1999. Processing and microstructural characterization of porous biocompatible protein polymer thin films. *Polymer* 40: 7397–7407.

37. Deitzel, J. M., J. Kleinmeyer, D. Harris, and N. C. B. Tan. 2001. The effect of processing variables on the morphology of electrospun nanofibers and textiles. *Polymer* 42: 261–272.

38. Matthews, J. A., G. E. Wnek, D. G. Simpson, and G. L. Bowlin. 2002. *Biomacromolecules* 3: 232.

39. Taylor, G. 1964. Disintegration of water drops in an electric field. *Proc. R. Soc. Lond. A* 280: 383–397.

40. Zhong, X. H., K. S. Kim, D. F. Fang, S. F. Ran, B. S. Hsiao, and B. Chu. 2002. Structure and process relationship of electrospun bioabsorbable nanofiber membranes. *Polymer* 43: 4403–4412.

41. Pawlowski, K. J., H. L. Belvin, D. L. Raney, J. Su, J. S. Harrison, and E. J. Siochi. 2003. Electrospinning of a micro-air vehicle wing skin. *Polymer* 44: 1309–1314.

42. Demir, M. M., I. Yilgor, E. Yilgor, and B. Erman. 2002. Electrospinning of polyurethane fibers. *Polymer* 43: 3303–3309.

43. Zhao, S. L., X. H. Wu, L. G. Wang, and Y. Huang. 2004. Electrospinning of ethyl-cyanoethyl cellulose/tetrahydrofuran solutions. *J. Appl. Polym. Sci.* 91: 242–246.

44. Jarusuwannapoom, T., W. Hongrojjanawiwat, S. Jitjaicham, L. Wannatong, M. Nithitanakul, C. Pattamaprom, P. Koombhongse, R. Rangkupan, and P. Supaphol. 2005. Effect of solvents on electro-spinnability of polystyrene solutions and morphological appearance of resulting electrospun polystyrene fibers. *Eur. Polym. J.* 41: 409–421.

45. Min, B., S. W. Lee, J. N. Lim, Y. You, T. S. Lee, P. H. Kang, and W. H. Park. 2004. Chitin and chitosan nanofibers: Electrospinning of chitin and deacetylation of chitin nanofibers. *Polymer* 45: 7137–7142.

46. Tomlins, P., P. Grant, P. Vadgama, S. L. James, and S. V. Mikhalovsky. 2004. *Structural characterisation of polymer based tissue scaffolds*, Report Number DEPC-MN-002. Teddington, Middlesex, UK: National Physical Laboratory.

47. Murugan, R., and S. Ramakrishna. 2006. Nano-featured scaffolds for tissue engineering: A review of spinning methodologies. *Tissue Eng.* 12: 435–447.

48. Hollister, S. J. 2005. Porous scaffold design for tissue engineering. *Nat. Mater.* 4: 518–524.

49. Huang, X. J., D. Ge, and Z. K. Xu. 2007. Preparation and characterization of stable chitosan nanofibrous membrane for lipase immobilization. *Eur. Polym. J.* 43: 3710–3718.